Titanium Aluminide Coating on Titanium Surface Using 3-Dimensional Micro Welder

Naoki. Mizuta[1)], Kiyotaka. Matsuura[2)]*, Soshu. Kirihara[3)], Yoshinari. Miyamoto[3)]

1) Graduate Student, Graduate School of Engineering, Hokkaido University, Sapporo, Hokkaido 060-8682, Japan

2) Graduate School of Engineering, Hokkaido University, Sapporo, Hokkaido 060-8628, Japan

3) Joining and Welding Research Institute, Osaka University, Ibaraki, Osaka 057-0047, Japan

* Corresponding author. Tel. /fax: +81 11 706 6343.

E-mail address: matsuura@eng.hokudai.ac.jp (K. Matsuura)

Abstract

Feasibility of a new method of titanium aluminide coating on titanium surface based on a reaction between aluminum liquid beads and the surface of titanium substrate has been studied using a computer aided 3-dimensional micro welder (3DMW) designed by the present authors. A predetermined length of thin aluminum wire was fed onto the substrate surface, and a spark was stricken from a thin electrode of a W-Ce_2O_3 alloy to make a small aluminum liquid bead on the substrate surface and to simultaneously melt a small area of the substrate surface beneath the bead. All conditions including the length of the wire feeding, the position of the electrode, electric power etc. had been programmed beforehand. The liquid bead containing aluminum and titanium rapidly solidified on the titanium substrate surface producing titanium aluminides on it. Repetition of the aluminum wire feeding, the electrode positioning and the spark striking produced a coating layer consisting of sub-layers of $TiAl_3$, TiAl and Ti_3Al from the surface side to the substrate side. Vickers hardness and wear resistance of the coated sample were remarkably improved.

Keywords: Surface modification, Titanium aluminides, TIG welding, CAD/CAM, Rapid prototyping

1. Introduction

Because intermetallics of titanium aluminides such as TiAl have many attractive chemical and mechanical properties [1], titanium aluminide coating on titanium surface will give good surface properties to titanium-based structural materials. Recently, several methods of titanium aluminide coating have been developed and studied [2-5]. However, some of them require plural processes, and some require advanced equipments, or in some cases the thickness of the coating layer or the bonding between the coating layer and the substrate is not enough for expecting

excellent chemical and mechanical properties of the coated material. Additionally, some of them require high treatment temperatures and long treatment time, which lead to the changes in microstructure and mechanical properties of the substrate. In this study, we have developed a simple coating method based on a conventional TIG welding technique. We designed a computer aided micro TIG welder called 3-dimensional micro welder (3DMW) and have studied on the three-dimensional freeform fabrication using the 3DMW [6-8]. This method using the 3DMW is a kind of rapid prototyping method based on CAD/CAM system. By pilling up of the bead, thicker coating layer will be obtained and using two different metal wires, three-dimensional elements distributions of the coating layer will be controlled. Additionally, coating area can be selected without masking process. In this study, we investigate the feasibility of aluminide coating on a titanium surface using the 3DMW.

2. Experimental Procedure

Figure 1 shows a photograph of the 3DMW. The 3DMW has a thin electrode made of a tungsten alloy, a water cooled stage and two wire feeders. The movement of the electrode and stage is controlled by a CAD/CAM file. A predetermined length of thin metal wire was fed onto the substrate surface from one or two metal wire feeders and sparks were stricken from the thin electrode to make a small liquid metal bead on the substrate surface and to simultaneously melt a small area of the substrate surface beneath the bead. By repeating the wire feeding and spark striking, relatively thick coating layer will be formed in a short time compared with a conventional coating method based on diffusion mechanism. Also, because only the surface of the substrate is melted, undesired microstructural change of the substrate material such as grain growth will be avoided.

Figure 2 shows schematic illustrations of the present coating method. The dimensions of the titanium substrate were 4mm x 20mm x 10mm. Its purity was 99.5 mass%. The surface was polished by a # 400 emery paper prior to the coating. Thin aluminum wire of 99.99 mass% purity was fed onto the surface of the titanium substrate and its tip was melted together with a small area of the titanium substrate surface by the spark to form an intermetallic liquid pool, which solidified into a small aluminide bead. The diameter of the aluminum wire, ϕ was varied from 0.2 to 0.3 mm. Figure 3 shows a schematic illustration of positions of the electrode and aluminum wire. The aluminum wire was supplied onto the substrate surface at a rate of L = 0.8 mm or 3 mm per spark. By combining the diameter and supplying rate of the wire, the volume of aluminum per spark was varied from 2.5 $x10^{-2}$ mm^3 to 2.2 $x10^{-1}$ mm^3. An electrode of the TIG welder was 1 mm in diameter and W-2mass%Ce_2O_3 in chemical composition. The tip of the electrode was sharpened forming a tip angle of 45 degrees. The distance between the electrode tip and the substrate surface, h was fixed at 1.2 mm. The electric voltage and current were 20 volts and 30 amperes, respectively, and the spark time was 180 ms. Argon containing 4 vol% of hydrogen was used as a shielding gas of the TIG welder. The mixed hydrogen gas functions as a reducer and heat conductive agent. Coating was performed by repeating the spark 200 times changing the position of the bead on the substrate surface. The 3DMW was controlled by a computer and it automatically coated the substrate surface.

After coating, the sample was slightly polished by using a #1500 emery paper and was analyzed by an X-ray diffraction (XRD) analyzer. Subsequently, a new surface near the bottom of the coating layer produced by grinding off the coating layer was also polished by the #1500 emery paper and was similarly analyzed. Another sample was sectioned perpendicularly to the coated surface and was polished. On the polished surface, metallographic observation and chemical analysis were performed using optical and scanning electron microscopes (OM, SEM) and an electron probe micro analyzer (EPMA). Concentration profiles of aluminum and titanium of the coating layer were investigated by the EPMA with the electron beam of 1μm diameter passing through the cross section from the surface to the substrate with 3μm inter-beam-point spacing. Vickers hardness profiles passing through the coating layer from the surface to the substrate were also investigated using an applied load of 50 g and a holding time of 30 s with 25 μm inter-indentation spacing. Wear resistance of the coating layer was evaluated using a pin-on-disk wear tester. The wear test specimen was titanium bar having a 5-mm diameter and a 15-mm length, which was cut from a commercial bar of 99.5 mass% purity. One end of the specimen was aluminide-coated using the present method. The wear test was performed using an FC20 cast iron at a sliding speed of 1.9 m/sec and under a contact pressure of 1.28 MPa.

3. Results and Discussion

3.1. Chemical Analyses

Figure 4 shows the results of the XRD analyses performed on two different surfaces of a sample: (a) the surface of the coating layer and (b) a new surface near the bottom of the coating layer produced by grinding off the coating layer. The volume of the aluminum wire fed on to the titanium substrate per spark was 9.4×10^{-2} mm^3 (0.2 mm diameter and 3 mm length). On the surface of the coating layer, $TiAl_3$ and TiAl diffraction peaks were detected. Although a TiO peak was also detected in Fig. 4 (a), this is from an oxidized area on the uncoated titanium substrate near the coating beads. Near the bottom of the coating layer, on the other hand, another intermetallic compound of Ti_3Al was detected, as shown in Fig. 4 (b). The XRD results showed that the coating layer consisted of three different intermetallic compounds and also indicated that from the bottom to the surface of the coating layer, the aluminum concentration was graded.

Figure 5 shows profiles of aluminum and titanium concentrations in the coating layer for three different feeding volumes of aluminum wire per spark ((a) ϕ=0.2 mm, L=0.8 mm, V=2.5×10^{-2} mm^3, (b) ϕ=0.2 mm, L=3 mm, V=9.4×10^{-2} mm^3 and (c) ϕ=0.3 mm, L=3 mm, V=2.2×10^{-1} mm^3). Three different chemical compositions were observed in the concentration profiles, namely approximately 75Ti-25Al, 50Ti-50Al and 25Ti-75Al in atomic percent. Judging from the XRD analyses, these compositions revealed that titanium aluminides of Ti_3Al and TiAl and $TiAl_3$ were produced in the coating layer. Figure 5 (b) indicates that the coating layer consists of TiAl, but it is likely that a very thin layer of $TiAl_3$ was formed on the surface of the TiAl layer, judging from the XRD result shown in Fig. 4 (a). As the volume of the aluminum wire per spark increased, the aluminide type changed from titanium-rich one to aluminum-rich one. The concentration profiles exhibited a step wise change in the thickness direction due to the discontinuous change in the

composition from one aluminide to another one. The Ti:Al ratio of the composition step increased as the distance from the surface increased. Beyond the interface between the coating layer and the titanium substrate, aluminum diffused into the titanium substrate and produced an aluminum-containing titanium-based solid solution.

3.2. Metallographic Observation

Figure 6 shows cross sections of the aluminide coatings. Thickness of the coating layer was ~300 μm. The coating layer can be divided into some parts having different brightness in the photograph. Judging from the EPMA and XRD results, (1) the coating layer shown in Fig. 6 (a) mainly consists of Ti_3Al, (2) the coating layer shown in Fig. 6 (b) consists of two aluminide phases of TiAl in the surface part and Ti_3Al in the bottom part, and (3) the coating layer shown in Fig. 6 (c) consists of three aluminide phases of $TiAl_3$, TiAl and Ti_3Al from the surface side to the bottom side. When the aluminum supply, *V*, was 9.4 $x10^{-2}$ mm^3 and when it was 1.1 $x10^{-1}$ mm^3, the coating layer consisted of a very fine dendritic structure, as shown in Figs. 6 (b) and (c), which indicates that the coating layer was formed by solidification of an alloy liquid. The solidification started from the interface between the coating layer and the substrate and grew upward to the surface, as shown in Figs. 7 (a) and (b). When the aluminum supply, *V*, was 2.5 $x10^{-2}$ mm^3, the Widmanstätten structure as shown in Fig. 8 was observed, which may be due to the βTi to Ti_3Al transformation during cooling after solidification.

The coating layer exhibited a contrast having a saw-edged shape as shown in Figs. 6 (a) and (b). The saw-edged shape was considered to have been originated from the discontinuous formation of the aluminide beads. It is likely that when a new aluminide bead was made very close to the former one, most part of the former bead was remelted. A series of the interfaces between the remelted and un-remelted parts appeared as the saw-edged shape. When the aluminum supply increased, cracks appeared in the coating layer, as shown in Figs. 6 (b) and (c). It was thought that the cracks were formed owing to a difference in the coefficient of thermal expansion (CTE) between the titanium substrate and the coating layer. For example, the mean CTE of titanium at temperatures from 273 to 923 K is 10 $x10^{-6}K^{-1}$ and that of TiAl at temperatures from room temperature to 873 is 13.7 $x10^{-6}K^{-1}$, respectively [9, 10], so tensile stress will be generated in the TiAl coating layer during cooling after solidification.

In Fig. 6, bright parts and dark parts are observed in the coating layer. Titanium was rich in the bright parts, while aluminum was rich in the dark parts. This inhomogeneity in composition produced in the coating layer is due to inhomogeneous supply of aluminum. Because the aluminum wire was very thin and had a very low melting point, it was difficult to control the melting length of the aluminum wire. The melting length of the wire changed sensitively every time. The difference in the melting length of the wire led to the rough surface of the coating layer as shown in Fig. 6. We are now trying to realize a smooth surface by changing the supplying method of the aluminum from wire feeding to hot dipping. Also we consider that reduction in cooling rate of aluminide beads may be effective to avoid the crack formation [11, 12].

3.3. Structure of Aluminide Coating

The structure of the coating layer is schematically illustrated in Fig. 9. On the surface of the coating layer, a very thin layer of $TiAl_3$ exists. A thick layer of TiAl is formed in the middle part, and a Ti_3Al layer in the bottom part. Beneath the Ti_3Al layer, aluminum containing titanium-based solid solution is produced due to the diffusion of aluminum into the titanium substrate. As the volume of the aluminum wire fed on to the titanium substrate increases, the structure of the coating layer changes from Ti_3Al to (Ti_3Al + TiAl) and further to (Ti_3Al + TiAl + $TiAl_3$). In the case of diffusional aluminide coating method investigated previously by the present authors, only a thin $TiAl_3$ layer of about 10 μm was formed on the titanium surface after heat treatment at 1073 K for 1 hour. On the contrary, in the present case of 3DMW process, a very thick layer having a graded structure consisting of $TiAl_3$, TiAl and Ti_3Al sub-layers was formed. The graded structure is schematically illustrated in Fig. 10. In the first bead of the coating layer, a concentration graded structure having titanium-rich part at the bottom area is formed on the titanium substrate. When the liquid bead solidifies, aluminum concentration of the residual liquid increases as the solidification front migrates from the bottom to the surface of the bead due to the macro segregation. Therefore, the titanium aluminide type varies from a titanium rich one to aluminum rich one from the bottom toward the surface. When the second bead was formed very close to the first one, most part of the first bead was remelted. A series of the interfaces between the remelted and un-remelted parts forms the saw-edged shape, as described in Section 3.2.

3.4. Mechanical Properties

Figure 11 shows hardness profiles in the coating layers for three different aluminum wire feeding conditions. Judging from Figs. 5 and 11, Vickers hardness numbers of Ti_3Al, Ti-rich TiAl, Al-rich TiAl and $TiAl_3$ layers are 700 - 800, 500 - 600, ~400 and 550 - 600, respectively. These values are much higher than that for the titanium substrate of 200. Furthermore, these values are also higher than those of annealed titanium aluminides: 253 for Ti-25Al, 295 for Ti-48Al (γ-phase), 367 for Ti-55Al (γ-phase) and 490 for Ti-75Al [13, 14]. Especially, there was remarkably improvement of the hardness of the Ti_3Al coating compared with annealed Ti-25Al. By the rapid cooling rate of the present coating method, a liquid pool having nearly Ti-25Al composition solidified into a super-saturated βTi bead. After the solidification, fine needle like Ti_3Al precipitated from βTi matrix. Due to solid solution hardening and precipitation hardening, hardness of the Ti_3Al coating was remarkably improved. It indicates that rapid cooling rate is effective for improving the hardness of these intermetallics. It is likely that these hardness improvements were coursed by refinement of microstructure due to the high cooling rate.

Figure 12 shows the results of the wear test. The volume of the aluminum wire fed on to the titanium substrate was 9.4×10^{-2} mm^3 (0.2 mm diameter and 3 mm length). The results shown in Fig. 12 clearly indicate that the coating layer has extremely excellent wear resistance compared with the uncoated titanium substrate. From the slopes of the lines in the figure, the wear rate of the uncoated sample was evaluated to be 2 μm/m; on the other hand, that of the coating sample was as low as 0.018 μm/m.

Thus, wear resistant aluminide coating on titanium was done using the 3DMW process. However, this process still

has some problems such as roughness of the coating surface and crack formation in the coating layer having an aluminum-rich composition. We have recently started a research to solve these problems using an aluminum feeding method based on aluminum plating on the titanium surface.

4. Conclusions

Titanium aluminide coating layers having a thickness of ~300 μm were formed on the surface of titanium substrate using the 3-dimensional micro welder, 3DMW. The aluminide coating layer had 2 or 3 sub-layers consisting of Ti_3Al, TiAl and $TiAl_3$. As the volume of the aluminum wire fed onto the titanium substrate surface per spark increased, the aluminide type changed from titanium-rich one to aluminum-rich one. Vickers hardness of the aluminide coated sample was 400 to 800 depending on the chemical composition of the aluminide, which was much higher than that of uncoated titanium substrate, 200. This increase in hardness brought about excellent wear resistance.

References

[1] A. Hirose, T. Ueda, K.F. Kobayashi, Mater. Sci. Eng., A160 (1993) 143-153

[2] K.A. Khor, Y. Murakoshi, M. Takahashi, T. Sano, J. Materials Processing Technology, 48 (1995) 413-419

[3] S.E. Romankov, A. Mamaeva, E. Vdovichenko, E. Ermakov, NIM in Physics Research, B237 (2005) 575-584

[4] S. Mridha, H.S. Ong, L.S. Poh, P. Cheang, Journal of Materials Processing Technology, 113 (2001) 516-520

[5] Si-Cheng Kung, Oxidation of Metals, 34 (1990) Nos. 3/4

[6] M. Terakubo, J. Oh, S. Kirihara, Y. Miyamoto, K. Matsuura, M. Kudoh, Mater. Sci. Eng., A402 (2005) 84-91

[7] M. Terakubo, J. Oh, Y. Miyamoto, K. Matsuura, M. Kudoh, Intermetallics, 15 (2007) 133-138

[8] M. Katou, J. Oh, Y. Miyamoto, K. Matsuura, M. Kudoh, Materials and Design, 28 (2007) 2093-2098

[9] S. Zinelis, A. Tsetsekou, T. Papadopoulos, The Journal of Prosthetic Dentistry, 90 (2003) 332-338

[10] W.J. Zhang, B.V. Reddy, S.C. Deevi, Scr. Mater., 45 (2001) 645-651

[11] M.C. Chaturvedi, Q. Xu, N.L. Richards, Journal of Materials Processing Technology, 118 (2001) 74-78

[12] M.A. Muñoz-Morris, I. Gil, D.G. Morris, Intermetallics 13 (2005) 929-936

[13] J.E. Payne, P.D. Desai, Properties of Intermatallic Alloys I. Aluminides, 1994

[14] I.A. Zelenkov, É.N. Osokin, Poroshkovaya Metallurgiya, 158 (1976) No. 2

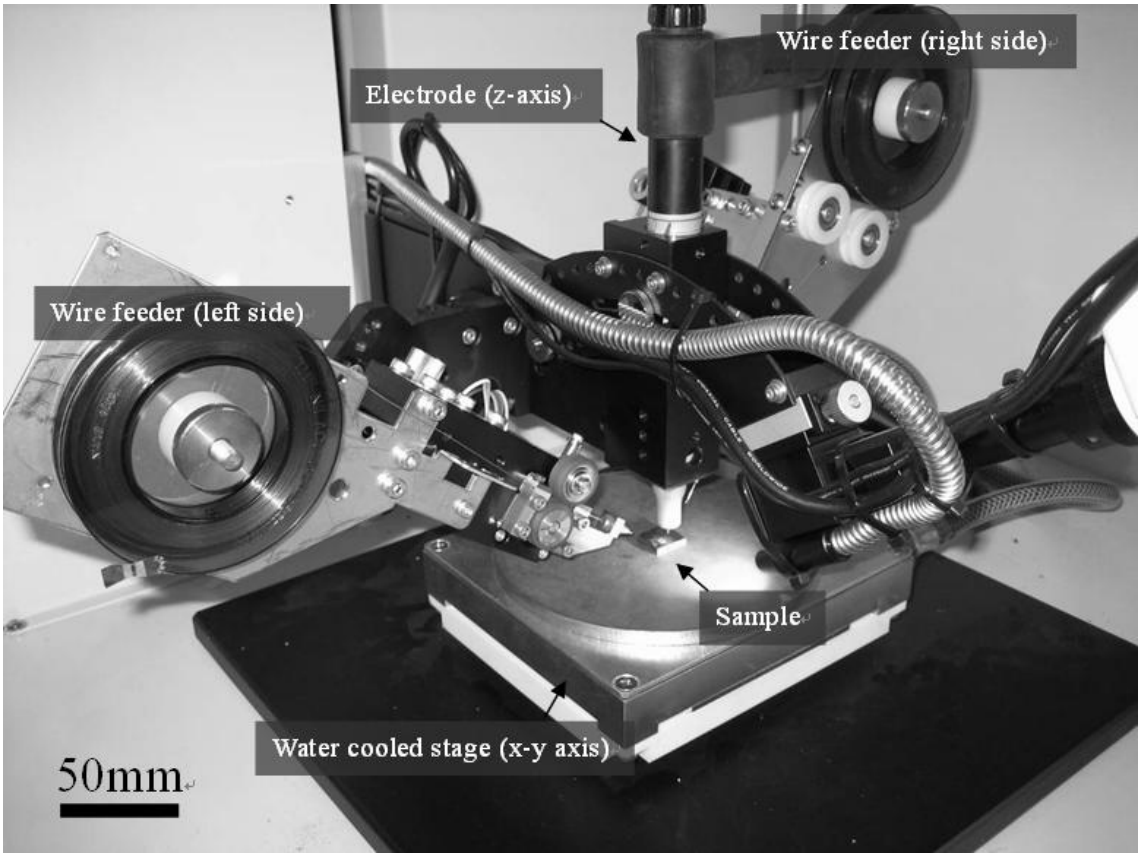

Fig. 1 3DMW equipment

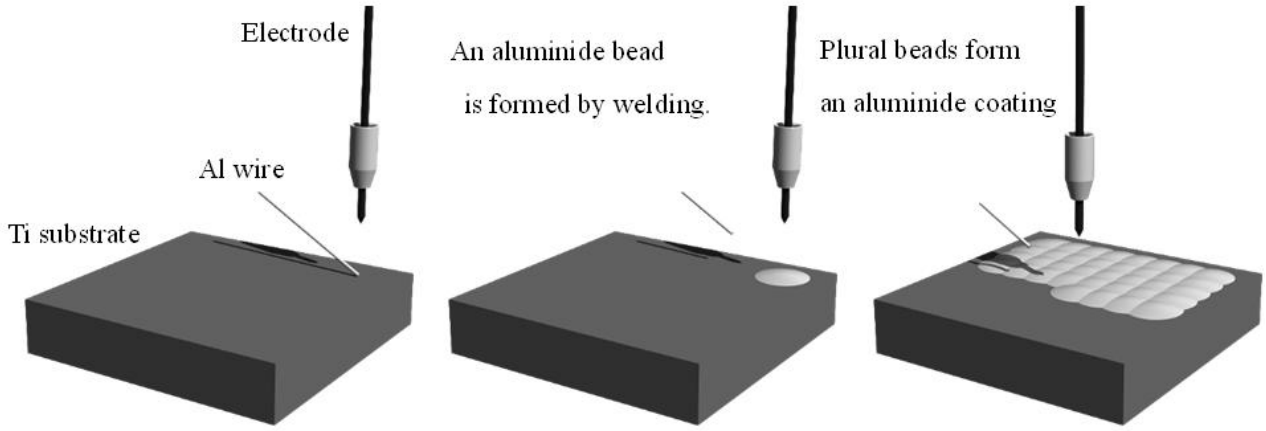

Fig. 2 Schematic illustration of the present coating method

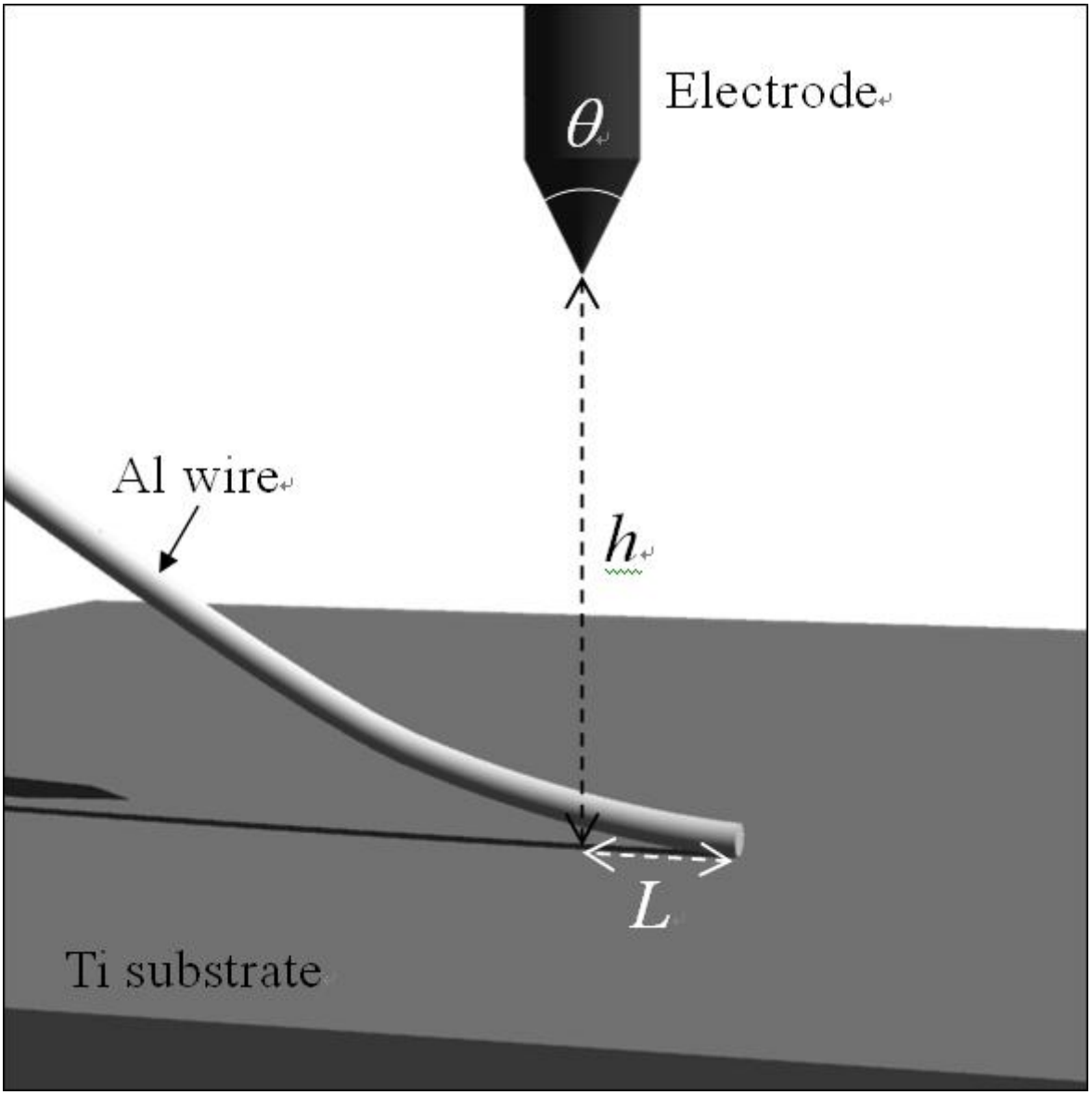

Fig. 3 Schematic illustration of positions of the electrode and aluminum wire

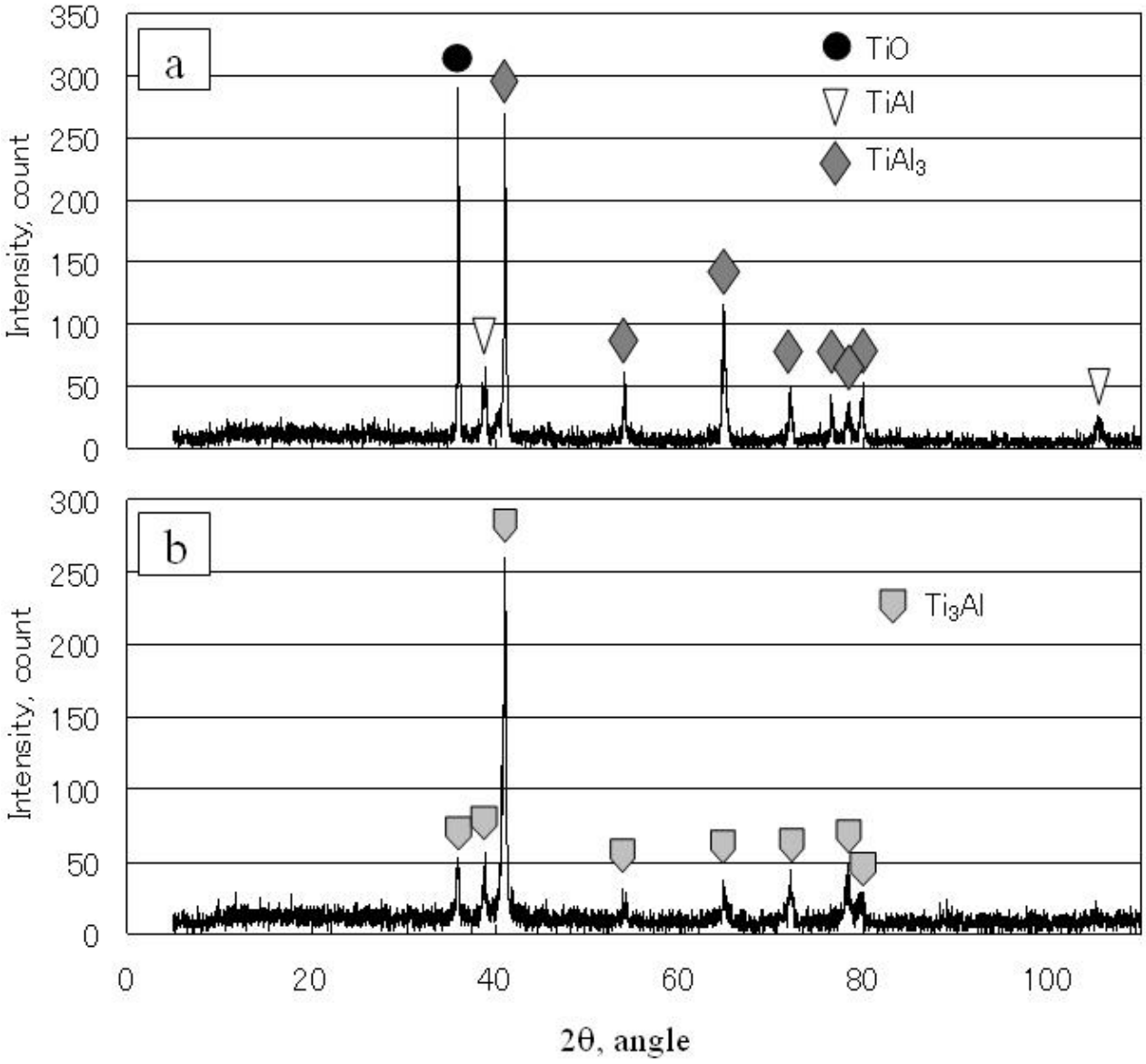

Fig. 4 Results of XRD analyses (ϕ=0.2 mm, L=3 mm, V=9.4x 10^{-2} mm^3)

Analyses were performed (a) on the surface of the coating layer and (b) on a new surface near the bottom of the coating layer produced by grinding off the surface layer.

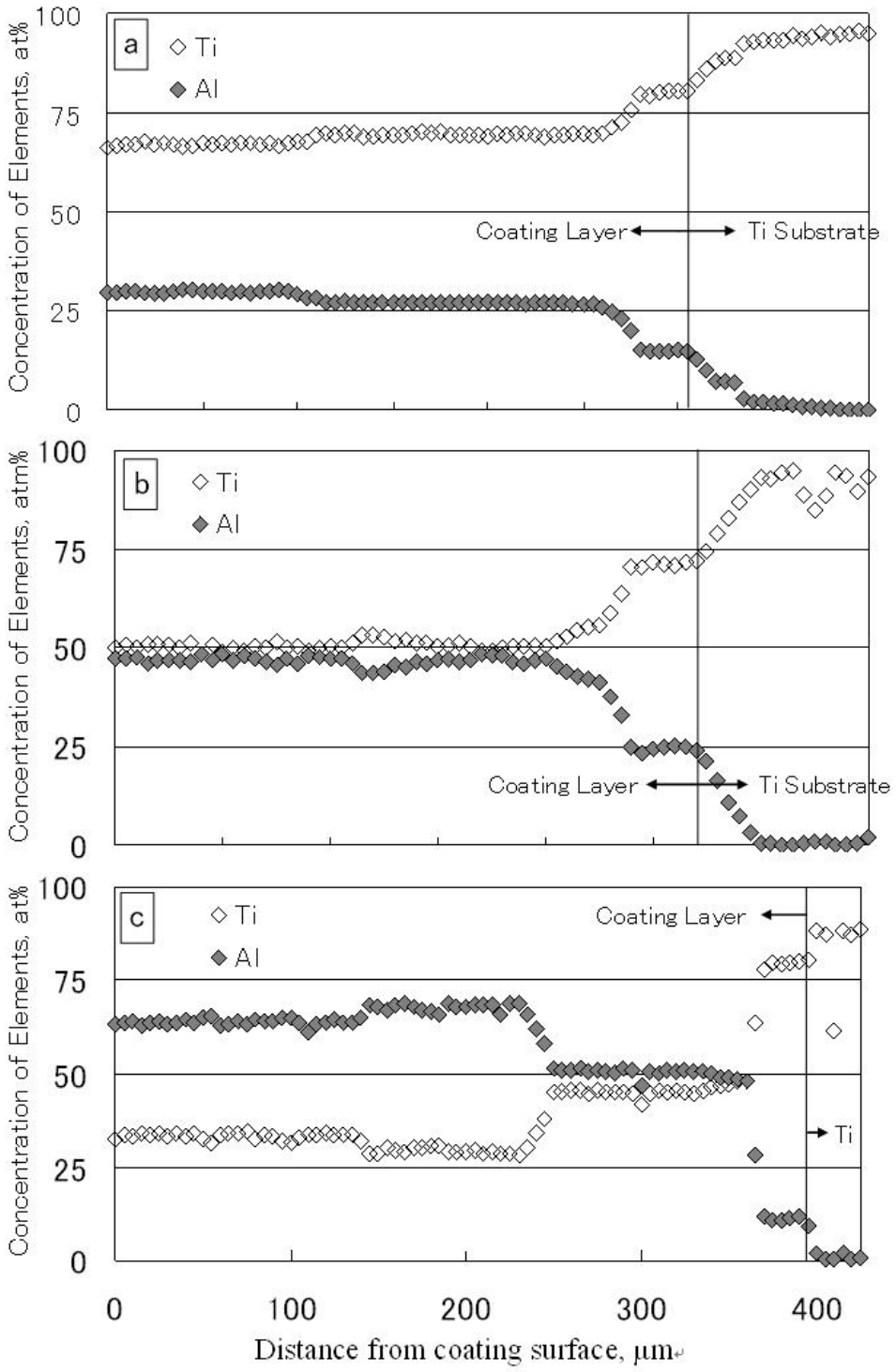

Fig. 5 Chemical concentration profiles in the coating layer

The diameter, ϕ, length, L, and volume, V, of the aluminum wire fed onto the titanium substrate were (a) ϕ=0.2 mm, L=0.8 mm, V=2.5 x10^{-2} mm^3, (b) ϕ=0.2 mm, L=3 mm, V=9.4 x10^{-2} mm^3 and (c) ϕ=0.3 mm, L=3 mm, V=2.2 x10^{-1} mm^3

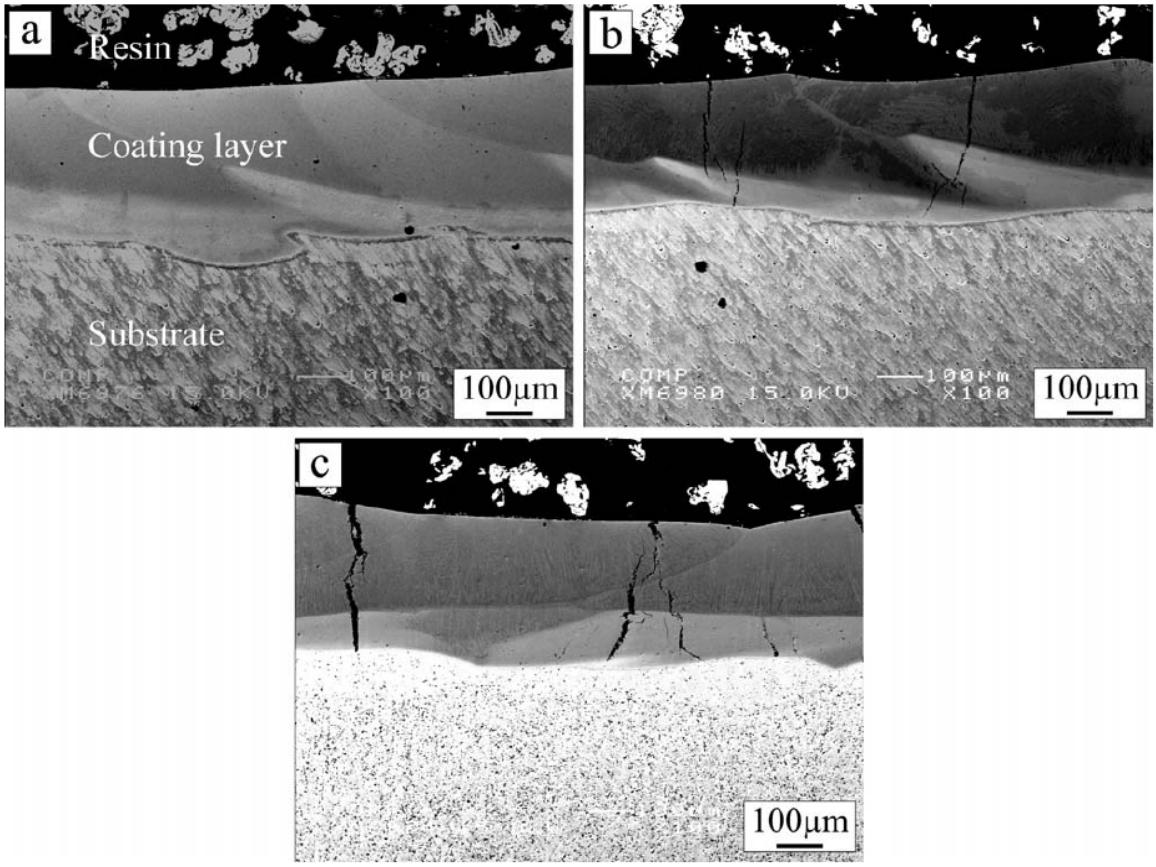

Fig. 6 Cross sections of coating layers (Backscattering electron image)

The diameter, ϕ, length, L, and volume, V, of the aluminum wire fed onto the titanium substrate were (a) ϕ=0.2 mm, L=0.8 mm, V=2.5 x10^{-2} mm^3, (b) ϕ=0.2 mm, L=3 mm, V=9.4 x10^{-2} mm^3 and (c) ϕ=0.3 mm, L=3 mm, V=2.2 x10^{-1} mm^3

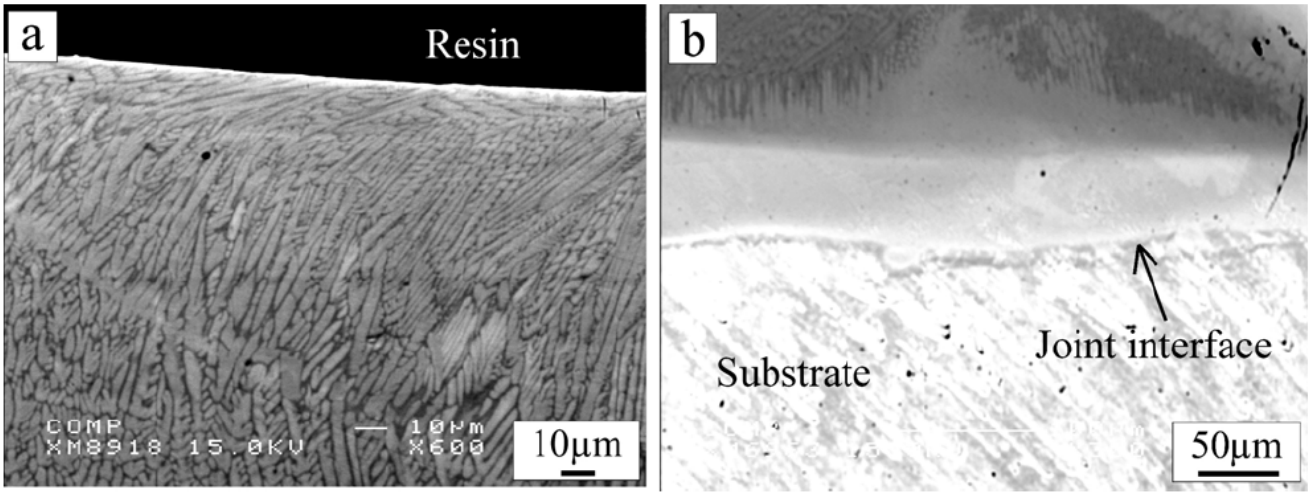

Fig. 7 Cross sections of a coating layer showing (a) dendritic microstructure in the surface part of the coating layer and (b) that in the bottom part. (Wire supply: ϕ=0.2 mm, L=3 mm, V=9.4 x10^{-2} mm^3 per spark)

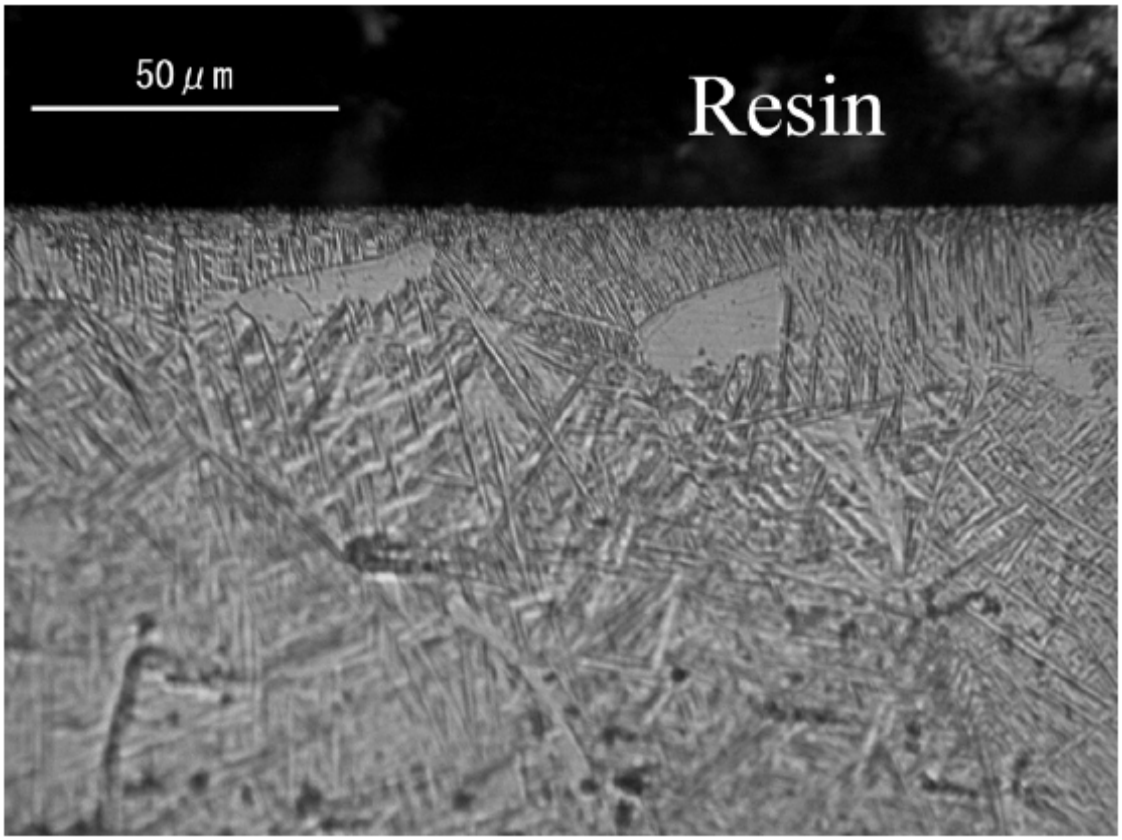

Fig. 8 Widmanstätten structure of the coating layer (Wire supply: ϕ=0.2 mm, L=0.8 mm, V=2.5 x10^{-2} mm^3 per spark)

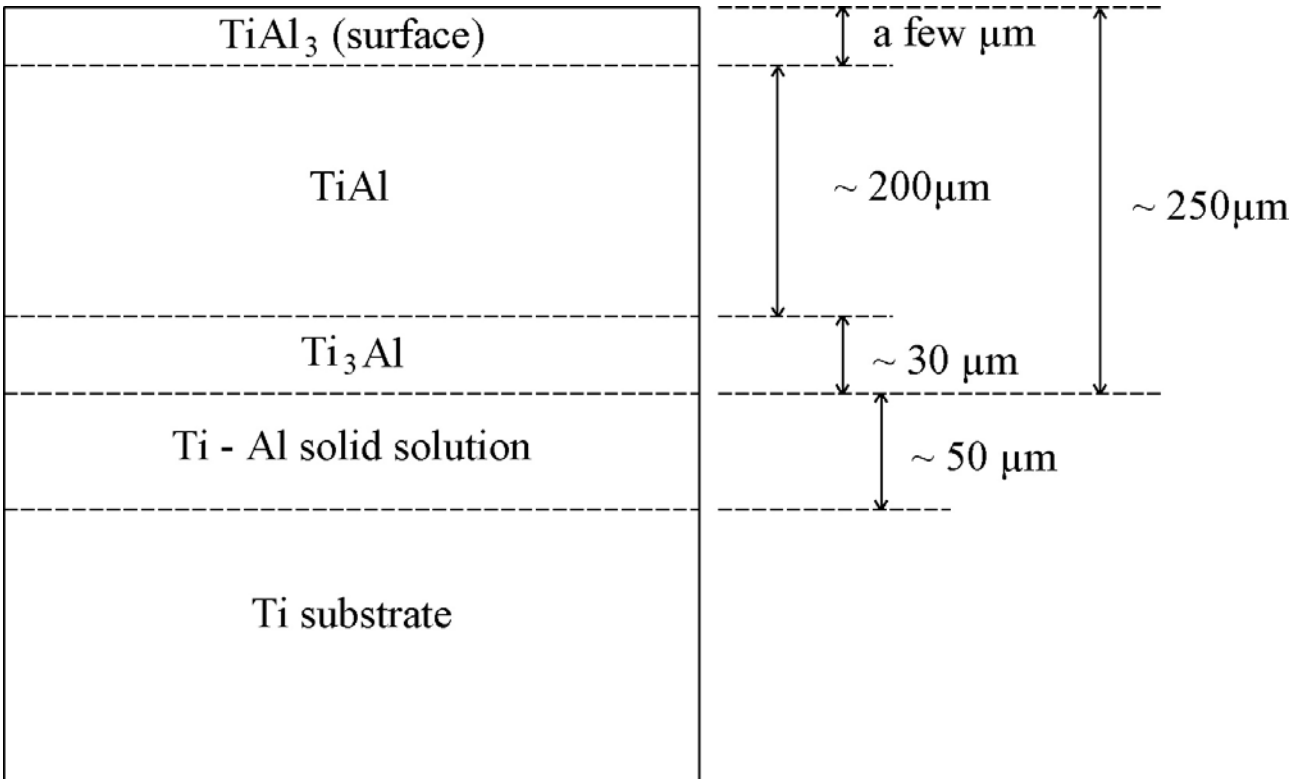

Fig. 9 Schematic illustration of the structure of the aluminide coating

ϕ=0.2 mm, L=3 mm, V=9.4 x10^{-2} mm^3

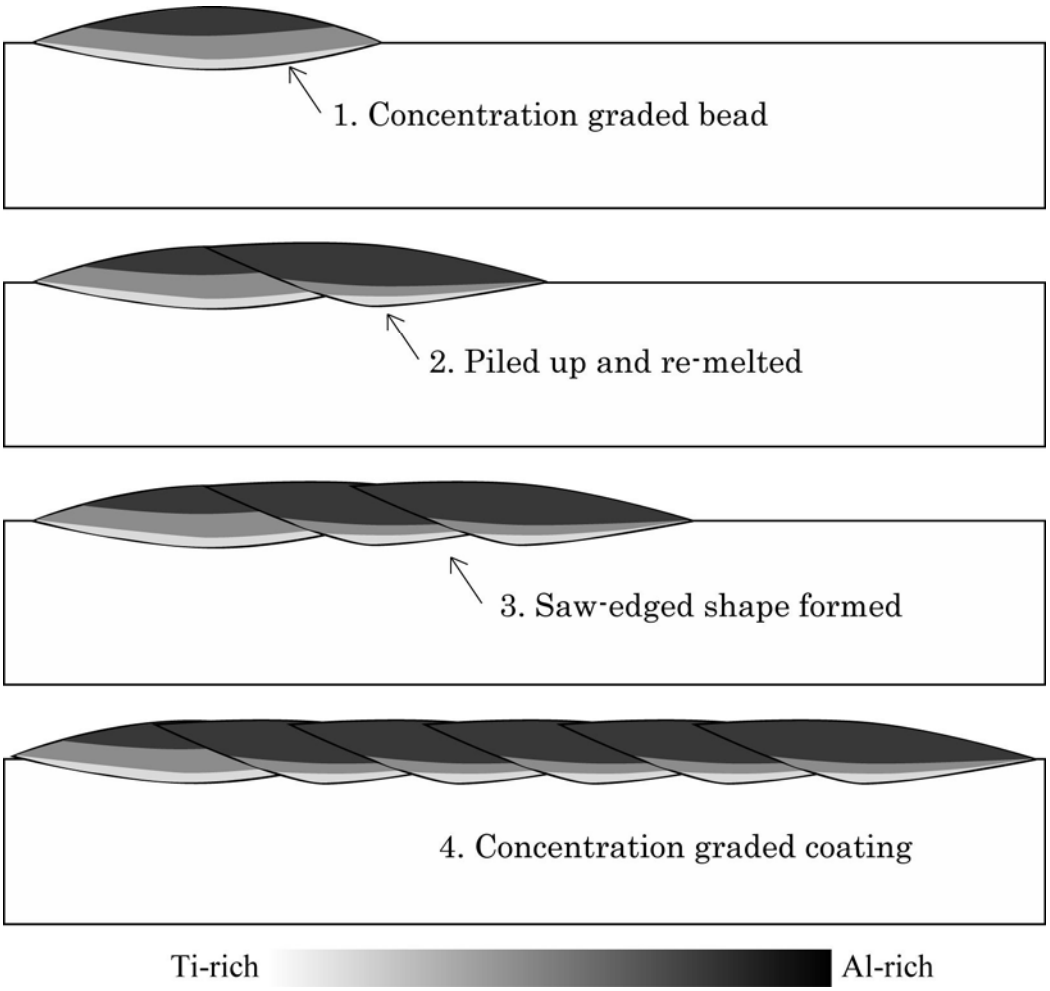

Fig. 10 Schematic illustration of the morphology of the graded coating structure

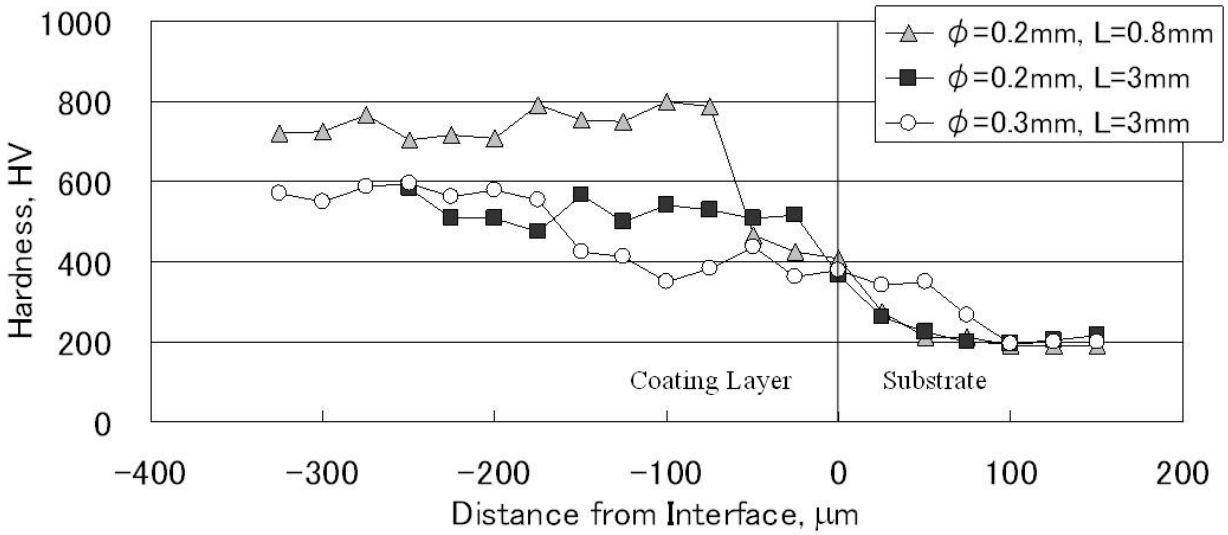

Fig. 11 Vickers hardness profiles of the coating layers

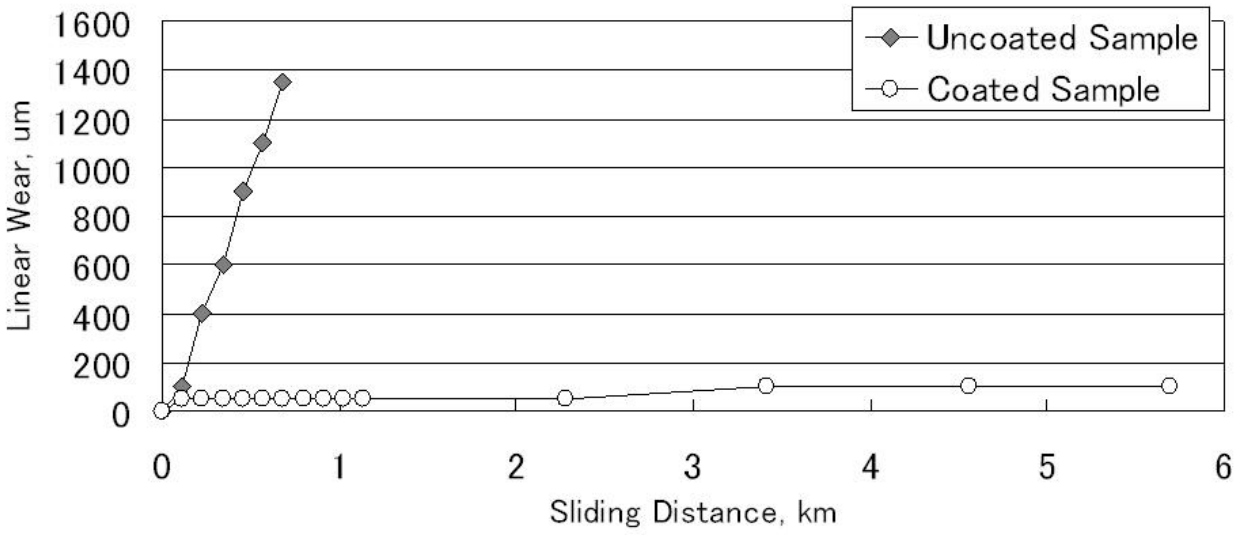

Fig. 12 Results of the wear tests

ϕ=0.2 mm, L=3 mm, V=9.4 x10^{-2} mm^3